



INTERNATIONAL ATOMIC ENERGY AGENCY
UNITED NATIONS EDUCATIONAL, SCIENTIFIC AND CULTURAL ORGANIZATION
INTERNATIONAL CENTRE FOR THEORETICAL PHYSICS
ICTP, P.O. BOX 586, 34100 TRIESTE, ITALY, CABLE: CENTRAFOM TRIESTE



H4.SMR/449-33

**WINTER COLLEGE ON
HIGH RESOLUTION SPECTROSCOPY**

(8 January - 2 February 1990)

EXTREME UV AND X-RAY LASERS

I.I. SOBEL'MAN

**Lebedev Physical Institute
Moscow 117925
U.S.S.R.**

EXTREME UV and X-RAY LASERS

I. I. SOBEL'MAN

1. Introduction
2. General Background
3. The Present Status of Short Wavelength Lasers
 - A. Collisional Pumping
 - B. Recombination Pumping
 - C. Other Pumping Schemes
 - D. Advances in X-Ray Optical Components
 - E. Future Applications of Soft X-Ray Lasers
4. Laser Produced Plasma as an Effective Source of Soft X-Ray Radiation

EXTREME UV and X-RAY LASERS

I. I. SOBEL'MAN

Lebedev Physical Institute Academy of Sciences of the USSR

1. Introduction

The problem of the short wavelength lasers was widely discussed last fifteen years. The numerous ideas for advancement in the extreme UV and soft X-ray regions and different experimental approaches were proposed for the purpose of creating population inversion and lasing between levels of multicharged ions in plasmas. Frequency upconversion and UV free-electron laser were also subjects of interest.

The first successful advancement in short wavelengths has been achieved using frequency upconversion. Examples of these results are the twentieth and twenty-eighth harmonics of neodymium glass laser, λ 52.2 nm and λ 38.0 nm, and the seventh harmonic of λ 240 nm Krypton fluoride excimer laser, λ 35 nm.

The most extensive theoretical and experimental studies have been devoted to creating inversion and lasing between levels of multicharged ions in plasmas. The main attention has been paid to laser produced plasma (LPP) (see [1-3]). It is connected with very important advantages of LPP as compared to other plasmas: the possibility to control plasma parameters electron temperature T_e , ion charge Z and electron density N_e in wide interval of values, to provide needed geometry of active medium varying the geometry of target irradiation (sharp point or linear focusing), to use different type of targets (massive targets, thin foils, multicomponent foils, fibers etc).

We discuss here the present status, perspectives and possible future applications of LPP lasers in extreme UV and soft X-rays. Attention is paid also to possible applications of LPP as a very effective point source of soft X-ray spontaneous radiation.

2. General Background

It seems helpful to begin with considering some specific features of the X-ray lasers which differ so much from the lasers in visible and near UV region.

In the case of visible lasers we can use laser cavities of very high quality. As a result it is sufficient to have the gainlength product $gL > 10^{-2}$. Therefore at $L = 10 \pm 100$ cm the gain should be $g > 10^{-3} \text{ cm}^{-1}$.

In the extreme UV of 100-40 nm a number of heavy metals have the reflection coefficient for normal incidence $R = 30 \pm 10\%$ respectively. For shorter wavelengths 30-10 nm due to recent progress in technology of multilayer periodical structures it becomes possible now to use multilayer mirrors with normal incidence reflectivity about 20-50%. No material has good enough transmission below 100 nm. Only a very thin films of some materials can be used as a transmitters or beam splitters.

The above mentioned progress in technology of normal incident multilayer X-ray optical components is so important to the problem of X-ray lasers that a brief review about recent achievements in this field is given farther in special section.

Normal incidence multilayer optical components can be used to produce laser cavities. But the quality of such cavities is not so high as in the visible spectral region.

As a result to have a real laser it is necessary to provide the active plasma medium with gain length product $gL > 10$.

As is shown below, low values of gain g as a rule cannot be compensated by large values of L because of plasma opacity and plasma refraction limitations. These limitations on active plasma length necessitate large value of g , much more larger than in visible spectra.

The multilayer optical components are available now for $\lambda > 10$ nm. We can hope to have such components for $\lambda > 5$ nm in the near future. For shorter wavelengths 5-1 nm lasing

can be demonstrated only by using superradiance. This means farther increase of needed gain g .

Consider now the gain coefficient g scaling with decreasing the laser wavelength λ . For a given transition of ions with charge Z , wave length λ is proportional to Z^{-2} .

Assuming the Doppler line broadening

$$\Delta\omega_D = \frac{\omega}{c} \bar{v} \propto T^{1/2} \lambda^{-1} \propto T^{1/2} Z^2$$

and taking into account that for the probability of the allowed electric dipole radiative transition $\lambda^2 A \sim \text{const}$ we have for the gain coefficient g along the isoelectronic sequences of ions

$$g \approx \frac{\lambda^2 A}{\Delta\omega_D} \Delta N \propto \frac{\Delta N}{N} \cdot N T^{-1/2} Z^{-2} \propto \frac{\Delta N}{N} N_z T^{-1/2} Z^{-2}$$

Here ΔN is the population inversion, N is the population of the upper level, proportional to the concentration of ions N_z . The temperature T needed to produce ions with charge Z is proportional to Z^2 . Assuming that $\Delta N/N = \text{const}$ we have

$$g \propto N_z Z^{-3} \propto N_e Z^{-4} \propto N_e \lambda^2$$

where N_e is the electron concentration in plasma. To keep $g = \text{const}$ while decreasing λ it is necessary to increase plasma electron density

$$N_e \propto Z^4 \propto \lambda^{-2}$$

Therefore the needed high value of gain g for short wavelengths can be provided only in hot ($T \propto \lambda^{-2}$) and dense ($N_e \propto \lambda^{-2}$) plasma.

We should take into consideration that population inversion can exist only for plasma density low enough that inelastic collisions do not dominate over radiative decay. In opposite case the Boltzmann equilibrium between the excited states takes place. The upper limit on plasma

density N_e^* is determined by equating probability of electron deexcitation $N_e^* \langle \nu \sigma \rangle$ to the probability of radiative decay A .

$$N_e^* \langle \nu \sigma \rangle \approx A$$

The rates of electron excitation and deexcitation are $\propto Z^{-3}$, the radiative probabilities $A \propto Z^4$. Therefore

$$N_e^* \propto Z^7, \quad N_z^* \propto Z^5$$

The maximum possible value of gain is

$$g_{max} \propto N_e^* Z^4 \propto Z^3 \propto \lambda^{-3/2}$$

Thus, at $N_e \sim N_e^*$ a needed high gain could be provided, but only if a very high input of energy is used to create plasma with necessary parameters

$$T \propto \lambda^{-1}, \quad N_e \propto \lambda^{-7/2}, \quad N_z \propto \lambda^{-3}$$

Note that the total energy E_z needed to create the ion with charge Z is of the order of $20 Z^{7/3}$ eV, and $N_z, E_z \propto Z^6, Z^{1/3}$

So a very significant increase in pumping power as compared to visible spectra is required. According to the scaling of gain g with decreasing the laser wavelength λ is necessary to increase N_e and pumping power by 7-8 orders of magnitude respectively.

As will be shown below existence of the inverse population in the case of multicharged ions usually is provided by a rapid radiative decay of the lower level and hence the radiation starting from the lower level should freely escapes, i.e. plasma must be optically thin in resonance lines, at least in transverse direction. Otherwise the lifetime of the lower level effectively increases and inversion is destroyed. In some inversion schemes the limitation on the transverse plasma dimension d is so strong that it practically eliminates the possibility of obtaining population inversion. For example, in He-like ions inversion between triplet and singlet states: $3^3S - 2^1P, 3^3D - 2^1P$ can be expected due to the large difference in radiative decay of 1P and $^3S, ^3D$ states. However, for a number of

transitions at λ 3-15 nm in He-like ions $Mg^{10+}, P^{13+}, Cl^{16+}$ the transverse plasma dimension should be $d < 10^{-3} L$.

In the case of very small transverse dimension d plasma is highly nonhomogeneous and the length L of lasing volume is limited by refraction.

The radius of the beam curvature R in nonhomogeneous plasma is given by

$$R^{-1} = \vec{e}_N \frac{1}{n} \nabla n$$

where \vec{e}_N is the unit vector of the principal normal to the beam, n is the index of refraction

$$n = \sqrt{1 - \omega_p^2 / \omega^2}, \quad \omega_p^2 = 4\pi N_e e^2 / m$$

and e and m are the electron charge and mass. For $\omega \gg \omega_p$

$$n \approx 1 - \frac{1}{2} \frac{\omega_p^2}{\omega^2}; \quad 1/\nabla n \sim \frac{\omega_p^2}{\omega^2} d^{-1}; \quad R \sim \left(\frac{\omega}{\omega_p} \right)^2 d$$

The maximum effective length of amplification in such nonhomogeneous plasma L is of the order $L < \sqrt{8Rd}$ or

$$L \approx \left(\frac{d}{10^2} \right) \left(\frac{10^{-6}}{\lambda} \right) \left(\frac{10^{22}}{N_e} \right)^{1/2}; \quad d [cm]; \quad \lambda [cm]; \quad N_e [cm^{-3}]$$

Assuming for example $\lambda = 10 \text{ nm} = 10^{-6} \text{ cm}$,

$d \approx 100 \mu\text{m} = 10^{-2} \text{ cm}$, $N_e \approx 10^{21} \text{ cm}^{-3}$ we have

$$L < 3 \text{ cm}$$

Because of the lack of high-quality laser cavities the required values of gain-length product gL needed for real laser in extreme UV and soft X-rays is $10^2 \approx 10^3$ times larger than gL in visible or usual UV spectra. This necessitates the use of very dense plasmas with electron concentration N_e of the order of the Boltzmann equilibrium limit N_e^* . The plasma with needed parameters for lasing at $\lambda \sim 10 \text{ nm}$ can be created by focusing a high-power laser beam on a solid target similar to that used in the experiments on laser controlled fusion, but very strong limitations on

plasma volume geometry are imposed by plasma opacity and refraction. These limitations are contradictory. To have plasma optically thin in resonance lines the transverse dimension d should be decreased. The decrease in d leads to plasma nonhomogeneity and as a consequence increases the refraction. The opacity and refraction limitations are very important from practical reasons. In some cases the experimental schemes optimal from the point of view of elementary processes responsible for inversion are not feasible because of these limitations.

The laser produced plasma (LPP) is expanding very rapidly. The duration of the active medium is of the order of nanoseconds. Additional problem is that the maximum abundance of ions with needed charge, created in transient plasma, should coincide in space and time with other needed plasma parameters.

So the problem of creating lasing LPP for short wavelengths $\lambda \sim 10\text{nm}$ is very complicated. As a result despite many different approaches suggested in theoretical works and treated experimentally, during many years no successful demonstration of lasing in LPP was obtained. The question arised whether the plasma parameters needed for lasing and assumed in theoretical estimations are provided under real experimental conditions of expanding LPP. Detailed computer simulation of plasma expansion and kinetics of ionization and recombination was necessary to answer this question. Only after computer codes for the analysis of atomic processes in LPP were developed consistently with the gasdynamics of plasma expansion we obtained the ground realistic predictions for experimental realization of the lasing plasma. In the next section we discuss the first successful attempt in this direction.

3. The Present Status of Short Wavelength Lasers

A. Collisional Pumping

The steady state population inversion on transitions $a \rightarrow b$ of different ions could arise in some interval of

electron temperatures and densities due to electron collisional excitation and rapid radiative decay of the lower level b . The population inversion on $3p-3s$ transitions of ions with ground electron configuration $(2p)^4$ due to electron collisional excitation of the $3p$ state and rapid decay of the $3s$ state is the example of this type.

For the simplest case consider the Neon like ion Ca^{19+} . The level diagram of this ion is shown in Fig. 1. The $2p^5 3s-2p^5$ and $2p^5 3d-2p^5$ transitions are the allowed electric dipole transitions. The states $2p^5 3p$ and $2p^5$ have the same parity and the electric dipole transitions from the states $2p^5 3p$ to the ground state $2p^5$ are forbidden. It is easy to show that population inversion on some of the $3p-3s$ transitions in optically thin plasma could be expected. Inversion exists as long as electron density and temperature are maintained at needed level, but the gain reaches its maximum value in very narrow interval of plasma parameters.

To provide the maximum concentration of Neon like ions the plasma temperature should not be too low or too high. The rate of electron collisional excitation rapidly increases with temperature. But if temperature is increased above some value the relative concentration of Ne-like ions decreases due to the next steps of ionization. The expected gain value is strongly influenced by reabsorption of $2p^5 3s-2p^5$ resonance radiation. So the transverse dimension of active plasma volume should not be too large. At the same time the refraction limitation on the transverse plasma profile is also very important. The similar considerations are valid for other ions of the Ne like isoelectronic sequence. The first experimental attempts to demonstrate lasing on $3p-3s$ transitions of Ne-like ion Ca^{19+} were made at Lebedev Physical Institute, Moscow (4).

The plasma active medium was created by linear focusing the radiation of the neodymium glass laser on the thin Ca target. The normal incidence resonator with diffractive output of radiation shown in the Fig 2 was used.

In rare photo, some evidence of lasing was reported. However, shot to shot reproducibility was not achieved because of the difficulty of providing all needed plasma parameters. Therefore the demonstration of lasing in these experiments is questionable and work was stopped with no real success.

The first absolutely incontrovertible demonstration of high gain and lasing in ultrasoft X-rays on the 3p-3s transitions of Ne-like ions has been achieved at Lawrence Livermore National Laboratory (LLNL) [5,6]. A very thin (75 nm) layer of selenium supported by thin polymer film (50 nm) has been used as a target.

Irradiated by two laser beams of neodymium glass laser Novette (power density $5 \cdot 10^{13}$ W/cm², pulse duration 450 psec) the target is uniformly heated. During the explosive expansion plasma contained Ne-like Se^{24+} ions forms practically homogeneous 200 nm thick layer. The uniform density in the central part of the plasma layer is very important from the point of view of refraction. The gain g 6 cm^{-1} has been observed for two transitions with λ 20.6 nm and λ 20.9 nm.

In farther experiments lasing has been demonstrated also on some transitions 3p 3s of other Ne-like ions Y^{29+} , Mo^{24+} [7] and Cu^{19+} , Ge^{22+} [8]. Mo^{22+} has produced a gain 4 cm^{-1} at λ 13.1 and λ 13.27 nm. The increase in pumping power density between Se and Mo is from $5 \cdot 10^{13}$ to $4 \cdot 10^{14}$ W/cm². It is easy to see that to use the same experimental technique for Ne-like ions with significantly larger charge Z requires a very powerful laser not available now.

The same scheme of excitation (collisional excitation) can be exploited also in the case of Ni-like ions. The level diagram for Ni-like ion Eu^{26+} is shown in Fig.3. The population inversion is produced on 4d 4p transitions. In LLNL experiments using more powerful Nova laser gains of order of 1 cm^{-1} has been observed on 4d 4p transitions

in Eu^{26+} λ 0.68 and λ 0.7 nm and in Yb^{27+} λ 0.026 and λ 0.6 nm [9], (see Table 1).

B. Recombination Pumping

Various electron processes preferentially fill the upper ion levels. The well known example is the three-body recombination in overcooled plasma. The lower excited levels are populated by cascade processes and depopulated by radiative transitions. This radiative decay is particularly fast for resonance level. In this way, a population inversion can occur for transitions $n=3-n=2$ and $n=4-n=2$ in H-like ions. Recombination as a pumping mechanism in neutral hydrogen plasma was proposed in the early 1960 s [10]. To advance to shorter wavelengths recombination in H-like ions has also been considered by many authors.

The possibility of using the transitions to the ground level during rapid cooling, when ground level is underpopulated, is very limited. The needed time of cooling falls drastically with increase of ion charge Z , Z^{-2} . For $Z=10$ must be shorter than 10^{-12} - 10^{-13} sec. Even for C^{5+} $\approx 10^{-12}$ sec. So the most promising is the inversion between excited levels arising due to collisional-radiative cascades accompanying the electron capture into highly excited states.

Population inversion in an expanding laser-produced plasma was reported in many experiments at different geometries of target irradiation and plasma expansion during 1970 s. (See 1-3). For example a significant gain on 3-2 transition in C^{5+} at λ 18.2 nm was observed during the rapid expansion of a carbon plasma created by the interaction of a laser beam with a very thin 4 μm diameter carbon fiber [11] [12].

The most impressive results are obtained in Princeton Plasma Physics Laboratory (PPPL) [13]. The soft X ray laser at PPPL is based on a rapidly recombining plasma confined in a magnetic field. The radiation of the CO_2 laser with

maximum pulse energy of 1 kJ and duration 70 nsec is focused onto a carbon disc located in a strong magnetic field, up to 90 kG, creating a plasma of sufficient temperature so that a substantial fraction of the ions are stripped of electrons. Radiation cooling of the plasma confined in a magnetic field after the laser pulse produces rapid three body recombination into highly excited states of H-like carbon. The population inversion on the transition $n=3 - n=2$, λ 18.2 nm, is formed because the level $n=2$ is rapidly depopulated by the strong $2 \rightarrow 1$ radiative transition. The level diagram of C^{5+} with level population processes and the scheme of experiment is shown in the Fig 4, Fig 5.

A very important essential of this experiment is magnetic field confinement. It enables to control the electron density, increases the plasma duration and forms the plasma into a long thin geometry suitable for a laser. An important feature is the radial profile of plasma shown in the Fig 5. The maximum population inversion is generated in an annular region around the centre of the cylindrical plasma.

A gain length product of $gL \approx 8$ at λ 18.2 nm has been achieved with an output energy of 1-3 mJ and beam divergency 5 mrad.

In a rapidly recombining plasma a population inversion can also been obtained in other ions, e.g. in Li like ions between levels 4f or 5f and 3d, due to the rapid radiative decay of level 3d [14, 15]. The small single pass gain on the transition 5f-3d in Al^{12+} , λ 10.5 nm has been observed in [16] (see also [16]).

C. Other pumping schemes

The main results obtained in demonstrating lasing in LPP as the amplifying media are shown in Table 2. According to this Table we have now different lasing transitions in H like, He like and Ne like ions at λ 20-10 nm. In all cases either collisional pumping or recombination pumping have been used. Some other inversion schemes have been also

discussed. Population inversion may be effectively enhanced by selective optical pumping using two plasmas, the first one as pumping plasma or plasma lamp and second plasma as an active medium. The upper level of the lasing ion Z_1 in an active medium is populated by an opacity broadened resonance radiation of ions Z_2 from pumping plasma ($Z_2 > Z_1$) [1, 18, 21].

There are also discussed the schemes in which the metastable and autoionizing levels can be used for storing pumped energy (see for example [22, 23]).

The lasers presently operating at λ 20-10 nm require a pumping laser energy of the order of 100 J [1] and power density up to 10^{14} W/cm². Taking into consideration the g value scaling with λ discussed above it is easy to estimate that using the same collisional and recombination pumping schemes the pumping laser energy for lasing at $\lambda \sim 1$ nm should be of the order of 1 MJ. Because the cost of a laser increased dramatically with energy a great deal of attention in X-ray laser development is devoted to some new schemes based on very short (picosecond and sub-picosecond) pumping pulses which provide high power density at not high pulse energy. The example of such scheme which has been considered in PPPL is shown in Fig 6 [17].

The approach uses two lasers. The first laser with relatively high energy is to create a plasma column of highly ionized ions Z confined in a strong magnetic field. It is possible to use either CO₂ laser with pulse energy ~ 0.5 kJ, and duration ~ 50 nsec, or neodymium glass laser with pulse energy ~ 100 J and duration ~ 3 nsec.

The next step is to excite one of the upper levels of the ion Z by multiphoton excitation or inner shell ionization using the laser with very high power density.

The picosecond or subpicosecond laser with pulse energy of the order of few joules could be used as a second laser. In [17] the KrF laser is considered for the role of extremely high power laser.

The progress in powerful subpicosecond laser system seems very promising for the further experiments in the field of short wavelength lasers.

D. Advances in X-Ray optical components

The progress in the field of the lasers with wavelengths shorter than λ 30 nm is very strongly influenced by recent successes in X-Ray optical components. In this spectral region no material transmits or reflects at normal incidence. Due to recent progress in technology of periodical structures and thin film deposition techniques the production of normal incidence multilayer interference mirrors and beam splitters is possible now. The different pairs of deposited layers Mo-Si, Au-C, Re-C, W-C are used for different wavelengths in soft X-rays providing normal incidence reflectivity about tens of percent. Figs 7 and 8 illustrate the performance of normal incidence mirrors and beam splitters around 13 nm [24]. The multilayer mirrors are spectral selective. The spectral resolution $\lambda / \Delta \lambda$ is determined by the number of deposited layers. The great achievement in X-Ray optics is the production of spherical multilayer mirrors.

As a result the usual approach to build laser cavity is used in design of soft X-ray laser systems.

E. Future applications of soft X-Ray lasers

If, as expected, laboratory soft X-Ray lasers are developed successfully in the next few years they will be very important instruments in different scientific and technological applications. Soft X-ray microscopy in biology, diffraction from crystals, material processing, including soft X-ray lithography, and atomic physics are usually quoted as the most likely fields of applications [31].

To illustrate the new possibilities offered by soft X-ray lasers we discuss briefly the soft X-ray microscopy. The great deal of attention is paid to this application in biology (see [17] [18]). Soft X-ray contact microscopy

offers a new method to obtain high resolution images of live cells. It is well known that to be viewed by an electron microscope the biological specimen must be dried and stained. Due to that some information about the living cell is lost. In soft X-ray microscopy the specimen placed on photoresist is contained in an environmental cell isolated from the vacuum system by a very thin ($\sim 0.1 \mu\text{m}$) silicon nitride window. The image is recorded on photoresist which is later viewed by an electron microscope. The highly collimated laser beam has some advantages as compared to conventional X-ray sources like synchrotrons of less blurring of the image and very short exposure time ($\sim 10 \text{ nsec}$) enabling flash images of live cells to be recorded. The several minutes of exposure are usually needed for synchrotron radiation.

The experimental scheme used in PPPL to develop the "Composite Optical Soft X-Ray Laser Microscope" (COXRLM) [25] is shown in Fig 9. The system was used in initial experiments to generate the contact images shown in Fig 10.

Only first initial steps in soft X-ray laser microscopy in biology were made up to this day but they are very promising.

It is very important for application in biology to develop the soft X-ray laser in "water window", which corresponds to the spectral interval between K edges of absorption of oxygen and carbon $\lambda < 4.4 \text{ nm}$. One of candidate for lasing in "water window" is 4d-4p transition in Ni-like ion W^{44+} , λ 4.315 nm [9].

4. Laser Produced Plasma as an Effective Source of Soft X-Ray Radiation

Soft X-Ray lasers discussed above are available now and will be available in near future only in some selected major laboratories where there are exceptionally powerful lasers for creating LPP with needed parameters. Therefore it is of interest to discuss what could be done in different applications using spontaneous soft X-ray radiation of LPP.

LPP with electron temperature $T_e = 100-1000$ eV and electron density $N \sim 10^{20}-10^{21} \text{ cm}^{-3}$ radiates very effectively in the soft X-ray spectral region. LPP with such parameters is created by sharp focusing onto a solid target powerful laser radiation providing flux density $q=10^{12}-10^{14} \text{ W/cm}^2$. The ions with charge $Z=10-40$ are created in LPP in dependence of the atomic number of target matter. The first, second, and third harmonics of neodymium glass laser with pulse energy of the order of joules or tens of joules and duration of the order of nsec are usually used in such experiments.

The typical parameters of LPP source of soft X-ray are shown in Fig 11 together with output intensity dependence on target atomic number. The efficiency of conversion of the initial laser pulse energy to the output soft X-ray energy is strongly dependent on initial laser wavelength. For the third harmonic of Nd-glass laser is one order of magnitude larger than for CO_2 laser. Under optimal experimental conditions for the targets with large atomic number $Z = 50-80$ the conversion efficiency may be as high as $\sim 50-70\%$.

The effective temperature of LPP radiation $T_R \approx 100-200$ eV could be provided. To increase T_R and some special targets are successfully used. In Fig 12 the example of such target is shown. The interior of gold spherical cavity with diameter 1 mm is irradiated by six beams of Gekko-XII laser providing power density $3 \cdot 10^{14} \text{ W/cm}^2$. The spectrum of the soft X-ray radiation in the range $1-5 \text{ nm}$ is similar to black body spectrum with temperature 200 eV (26). One of the most important disadvantages of LPP as a source of X-ray was that LPP radiates in solid angle 2π . After the spherical multilayer mirrors for soft X-rays became available the situation changed drastically. It is possible now to collimate or to focus the spontaneous radiation of LPP significantly increasing the power density on the sample placed on some distance from LPP as is shown in Fig 13. The scheme of experiment in which the power density of the LPP radiation

focused on a distant sample has been measured is shown in Fig 14, 15. Note that soft X-ray output is high enough even for comparatively low energy of laser pulse, corresponding to the YAG laser with pulse repetition frequency \sim few Hertz.

In Fig 18 some other version of experiment using focusing multilayer mirror is shown. Slightly tilting one of the mirrors it is possible to displace corresponding maximum of reflection in such way that radiation of $\text{C}^{K\alpha}$ $\lambda 18.2 \text{ nm}$ is reflected only by one mirror.

In conclusion it is of interest to compare the LPP as a source of soft X-ray radiation with synchrotron. This comparison is shown in Fig 17.

REFERENCES

1. P.L.Hagelstein Plasma Physics 12, 1345 (1983);
in Atomic Physics 9, edited by R.S.Van Dyck and
E.M.Fortson, World Scientific Publishing Co Pte
Ltd, (1984).
2. I.I.Sobel'man and A.V.Vinogradov Advances in Atomic and
Molecular Physics edited by D.Bates and B.Dederson 20 327
(1985).
3. M.H.Key Nature 316, 314 (1985).
4. A.A.Iljukhin et al. JETP Letters, 25, 536 (1977).
5. M.D.Rosen et al. Phys. Rev. Lett. 54, 106 (1985).
6. D.L.Matthews et al. Phys. Rev. Lett. 54, 110 (1985).
7. B.L.MacGowan et al. J. Appl. Phys. 61, 5243 (1987).
8. T.M.Lee et al. Phys. Rev. Lett. 59, 1185 (1987).
9. B.J.MacGowan et al. Phys. Rev. Lett. 59, 2157 (1987).
10. L.I.Gudzenko, L.A.Shelepin. Sov. Phys. JETP, 18, 998
(1964).
11. R.J.Dewhurst et al. Phys. Rev. Lett. 37, 1265 (1976).
12. D.Jacoby et al. Opt. Commun. 37, 193 (1981).
13. S.Suckewer et al. Phys. Rev. Lett. 55, 1753 (1985).
14. W.T.Silfvast et al. Appl. Phys. Lett. 39, 212 (1981).
15. G.Jamelot et al. in Proc. Int. Conf. Lasers'81, New
Orleans, LA, Dec. 1981, p. 178.
16. P.Jaegle et al. J.Opt. Soc. Am. B 4, 563 (1987).
17. C.H.Skinner et al. in X-Ray Microscopy II, Springer-
Verlag, p. 36, (1987).
18. A.V.Vinogradov et al. Sov. J.Quant. Electron. 2, 59
(1975).
19. B.A.Norton, M.J.Peacock. J.Phys. B 8, 989 (1975).
20. V.A.Bhagavatula. J. Appl. Phys. 47, 4535 (1976).
21. J.Milsen. Opt. Commun. 72, 371 (1989).
22. H.C.Kapteyn et al. Phys. Rev. Lett. 57, 2939 (1986).
23. S.Harris et al. Opt. Lett. 12, 331 (1987).
24. N.M.Ceglio. in X Ray Microscopy II, Springer Verlag,
p. 130 (1987).

25. D.S.DiCicco et al. Princeton Plasma Physics Laboratory,
Tech. Rep. PPPL 2596 (1989).
26. T.Mochizuki et al VII Internat. Conf. on Plasma Physics
and controlled Nucl. Fusion Research, Kyoto, Japan 1986.

Short-wavelength laser experiments.

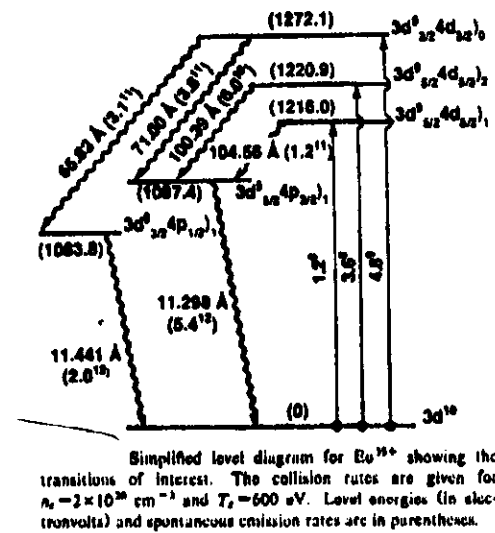
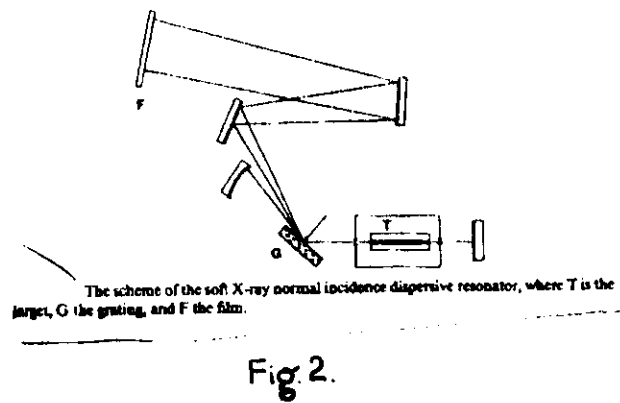
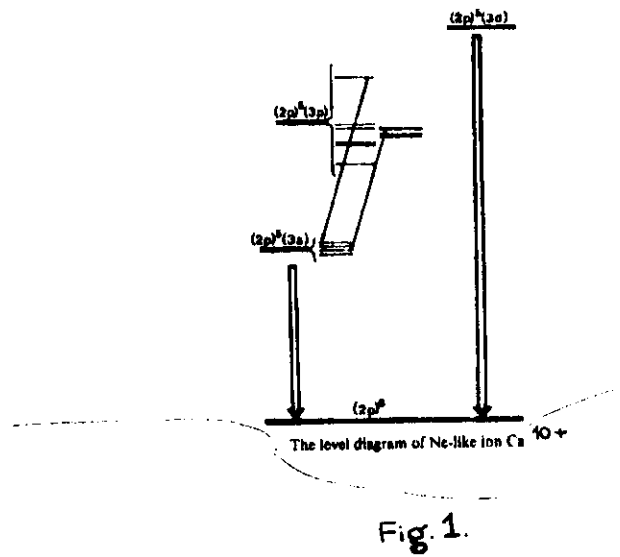
Table 2.

| Lab. | λ , Å | ion | transition | g , cm ⁻¹ |
|-------------------|---|-------------------------|----------------|-----------------------------------|
| LLNL 1985 | 206.3 209.6 | Se XXV [Ne] | 3p-3s | 5.5 |
| | 155.0 157.1 | Y XXX [Ne] | 3p-3s | - |
| Princeton 1985 | 182 | C VI [H] | 3 → 2 | $g \sim 6.5$ |
| Orsay 1985 | 105.7 127.9 | Al XI [Li] Mg X [Li] | 5f-3d 5f-3d | ~1 (3) ~1 |
| Rochester 1985 | 182 | C VI [H] | 3 → 2 | 3 |
| LLNL 1985 | 106.4 131.0 132.7 139.4 141.6 | Mo XXXIII [Ne] | 3p-3s | 0.8 2.0 1.3 0.16 0.16 |
| NRL 1987 | 221.11 279.31 284.67 | Cu XX [Ne] | 3p-3s | 2 1.7 1.7 |
| | 196.06 232.24 236.26 | Ge XXIII [Ne] | 3p-3s | 3.1 4.1 4.1 |
| RAL 1987 | 182 | C VI [H] | 3 → 2 | 3 |
| LLNL 1987 | 65.83 71.00 | Eu ³⁵⁺ [Ni] | 4d-4p | 0.6 1.1 |
| | 50.26 56.09 | Yb ⁴²⁺ [Ni] | 4d-4p | ~1 |
| RAL 1987 | 182 80.91 | C VI [H] F IX [H] | 3 → 2 3 → 2 | 4.1 3 |

LLNL = Lawrence Livermore National Laboratory
 Princeton = Plasma Physics Laboratory, Princeton University
 Orsay = University Paris-Sud
 Rochester = University of Rochester
 NRL = Naval Research Laboratory
 RAL = Rutherford Appleton Laboratory

| Wavelength | Measured Gain | Lasing Medium | Gain Length Demonstrated | Output Power Demonstrated |
|------------------|--------------------|---------------|--------------------------|---------------------------|
| 206.3 Å; 209.6 Å | 6 cm ⁻¹ | Ne-like Se | $\alpha L = 20$ | 10 ⁶ watt |
| 106.4 Å | 2 cm ⁻¹ | Ne-like Mo | $\alpha L = 6$ | 10 ³ watt |
| 131 Å; 132.7 Å | 4 cm ⁻¹ | | $\alpha L = 12$ | 10 ⁵ watt |
| 71 Å | 1 cm ⁻¹ | Ni-like Eu | $\alpha L = 4$ | 10 ³ watt |
| 50.3 Å | 1 cm ⁻¹ | Ni-like Yb | $\alpha L = 4$ | 10 ³ watt |

Table 1.



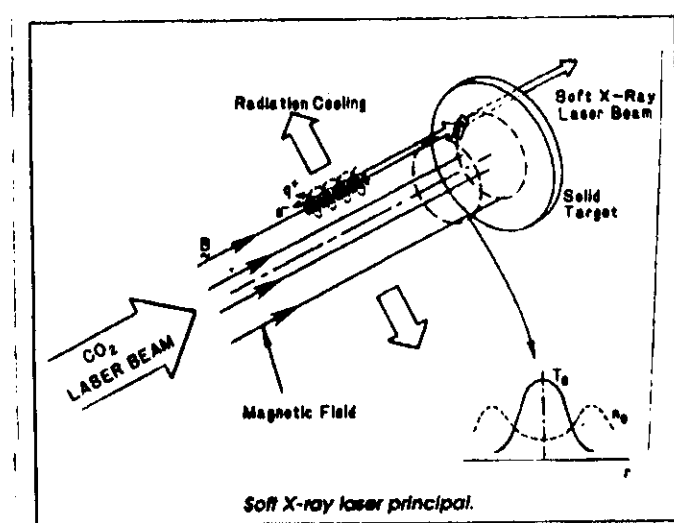
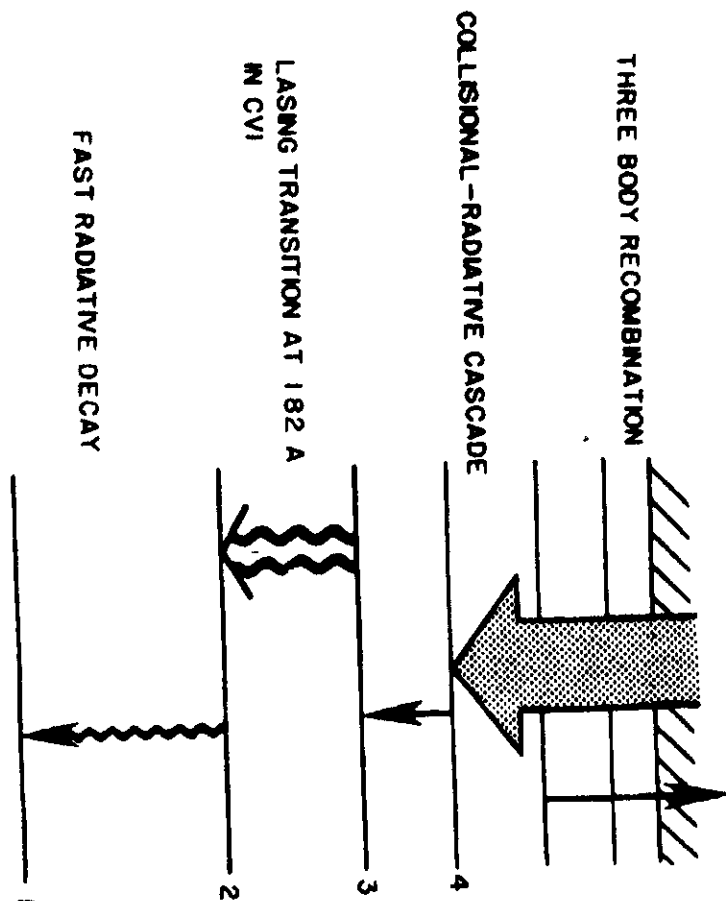


Fig 5.



TWO LASER APPROACH TO LASING IN 10 Å REGION

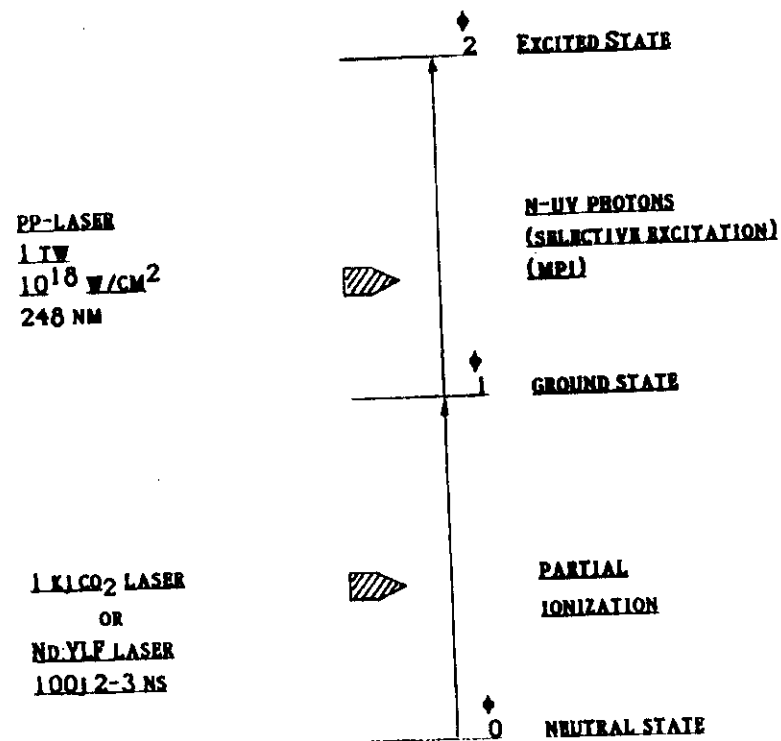


Fig. 6.

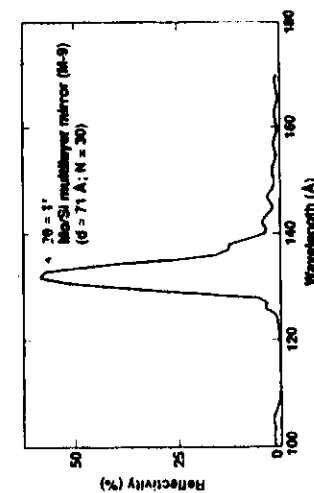


Fig. 7.

X-ray beamsplitter performance around $\lambda = 130\text{\AA}$

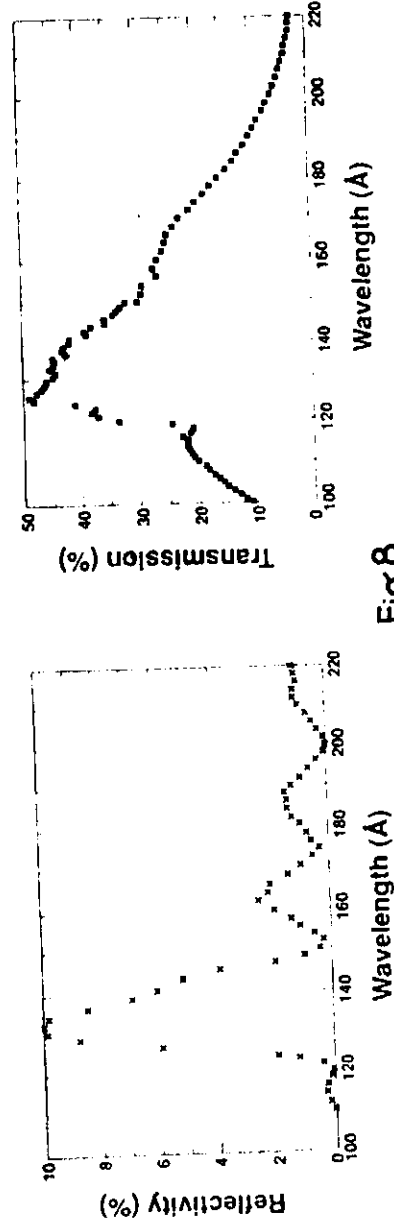
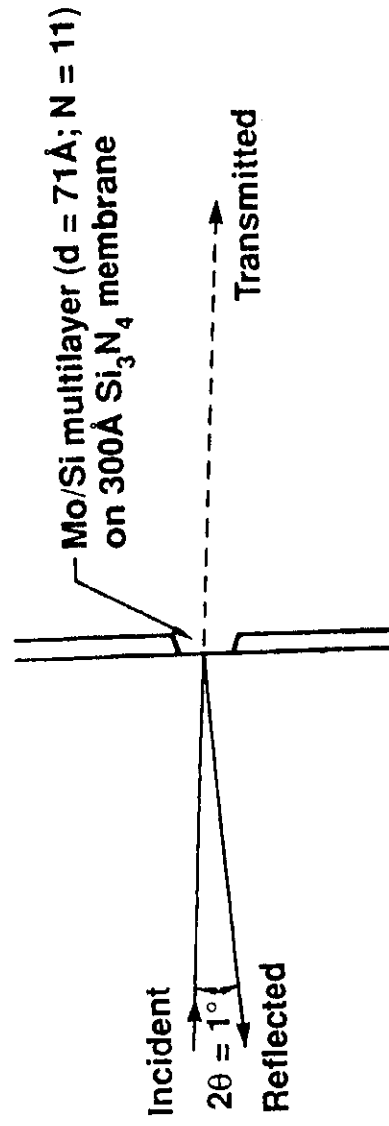


Fig. 8.

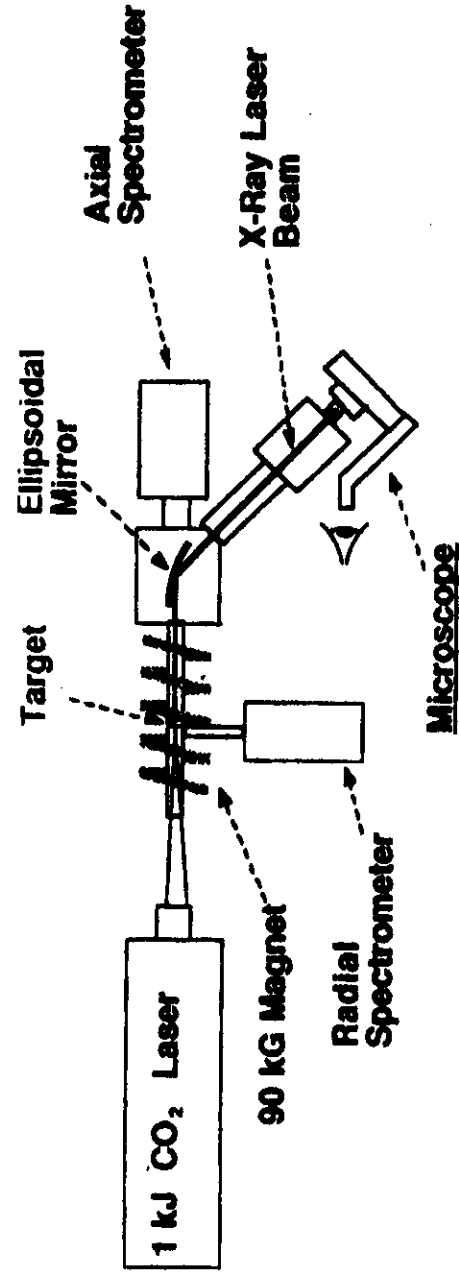


Fig. 9.

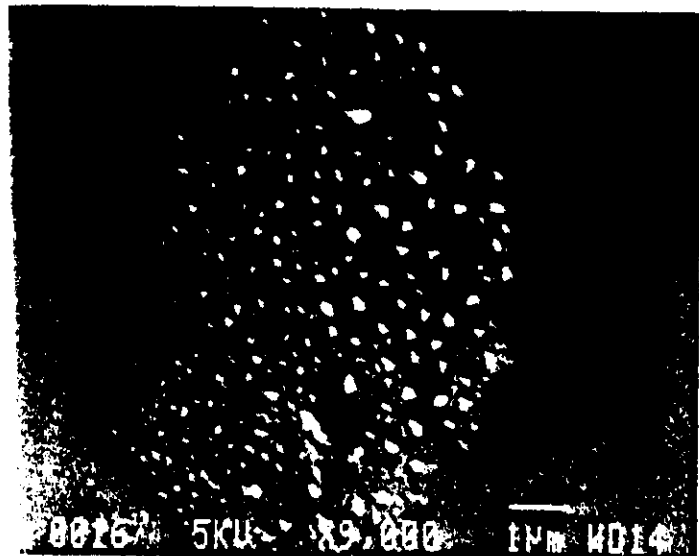
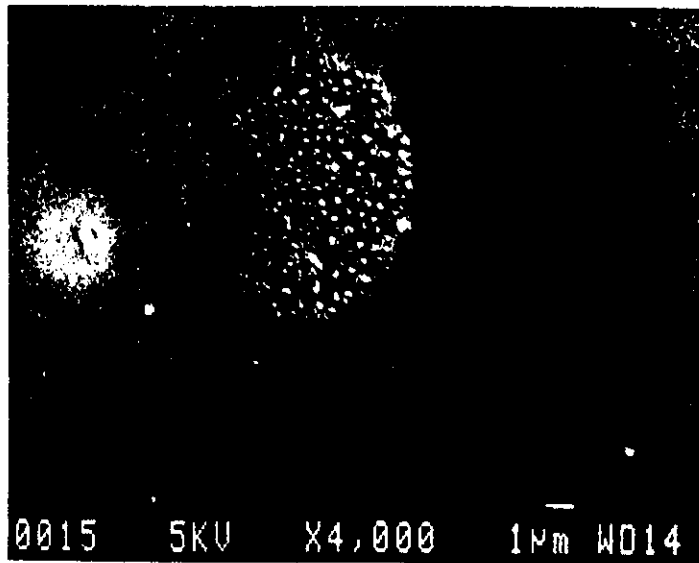
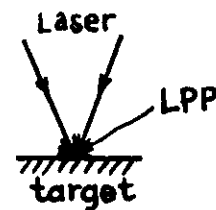


Fig. 10.

Laser produced plasma (LPP)



$$q_L = 10^{13} \div 10^{15} \text{ W/cm}^2$$

$$T_e \sim 1 \text{ keV}$$

$$N_e \sim 10^{21} \text{ cm}^{-3} \text{ for } \lambda_L = 1.06 \mu\text{m}$$

$$Z = 10 \div 30$$

experiment: spectral radiant power
absolutely measured x-ray spectra
x-ray conversion efficiency $\eta = E_{\text{x-ray}}/E_L$

for $q_L = 10^{13} \div 10^{15} \text{ W/cm}^2$,
high Z_A target, $\lambda = 10 \div 300 \text{ \AA}$

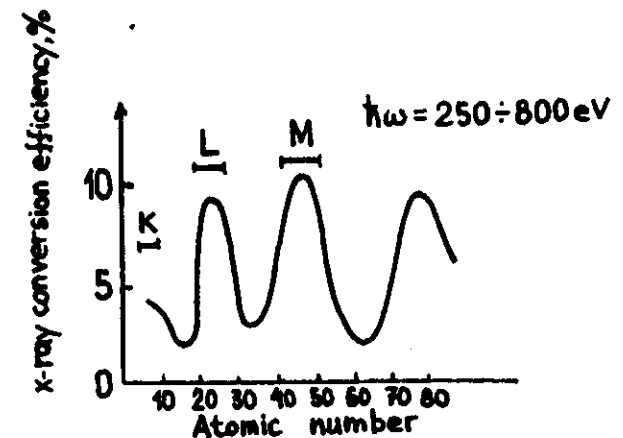
LPP - effective source of soft X-ray

$$r \sim 100 \mu\text{m}$$

$$T_R \sim 100 \text{ eV}$$

$$\eta = 0.1 \div 0.7$$

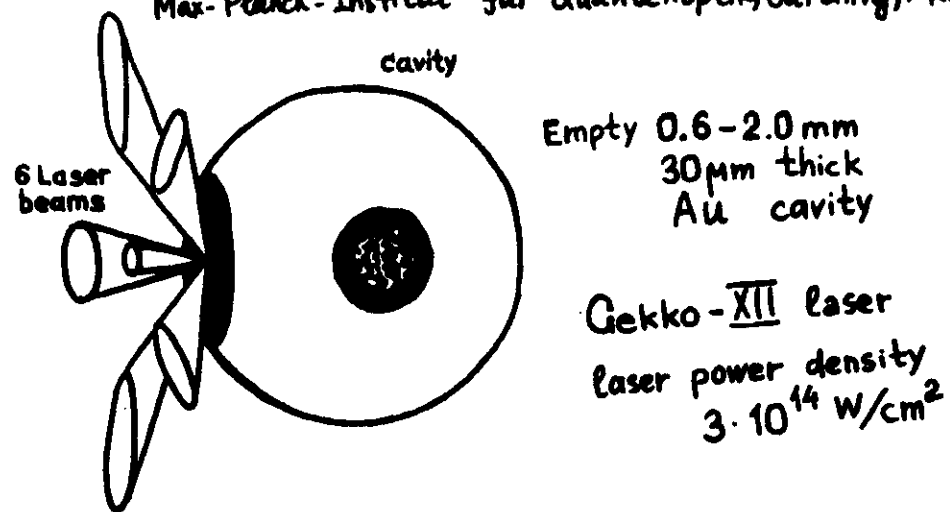
$$\hbar\omega \gtrsim 100 \text{ eV } (\lambda \lesssim 100 \text{ \AA})$$



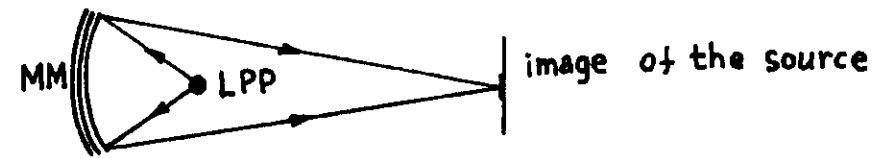
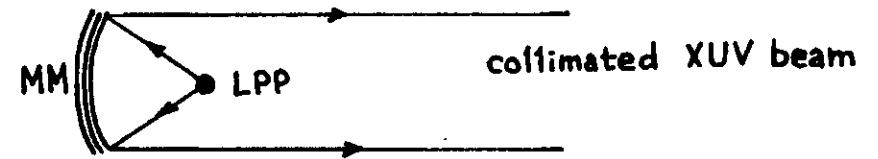
$$\text{Laser: } q = 7 \cdot 10^{12} \text{ W/cm}^2$$

$$7 \text{ J} / 15 \text{ ns} / 0.53 \mu\text{m}$$

(H.C. Gerritsen et al
J. Appl. Phys. 59, 2337 (1986))

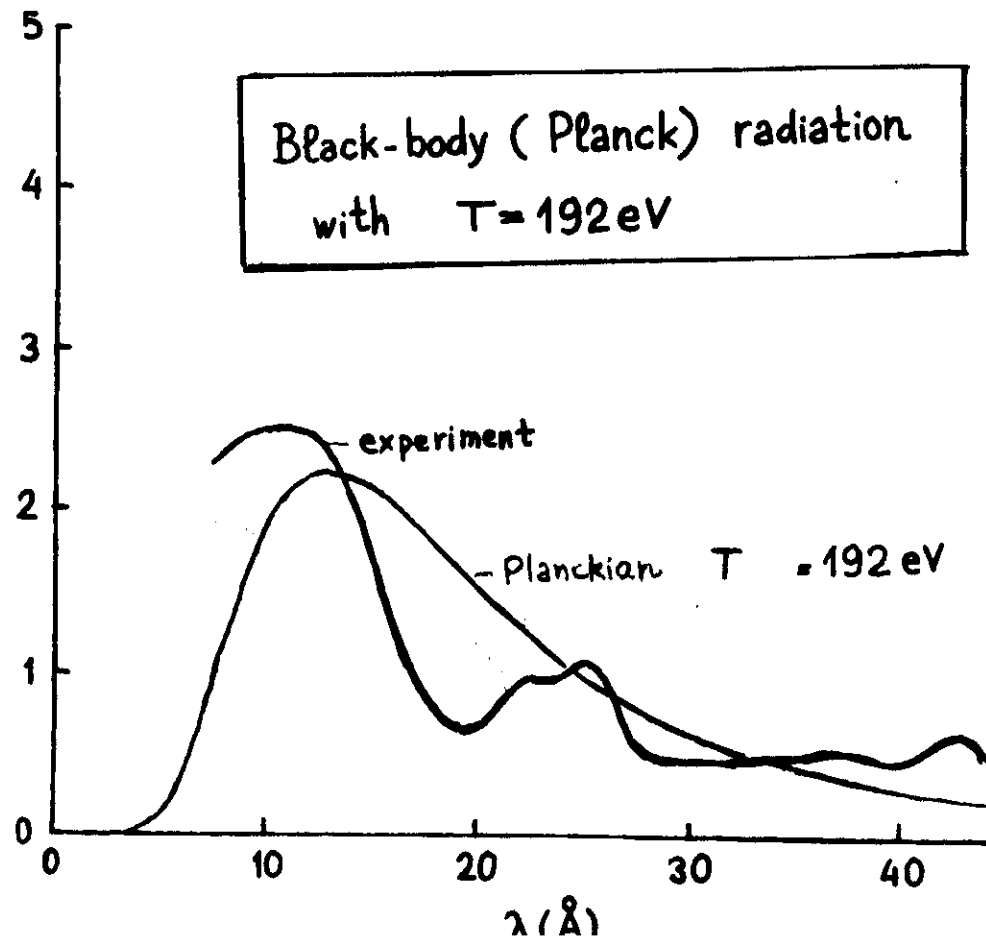


Formation of intense XUV radiation from LPP



MM = multilayer mirror
LPP = laser-produced plasma

Fig. 13.



FORMATION OF INTENSE COLLIMATED XUV RADIATION FROM LASER PRODUCED PLASMA BY MULTILAYER MIRRORS

EXPERIMENT

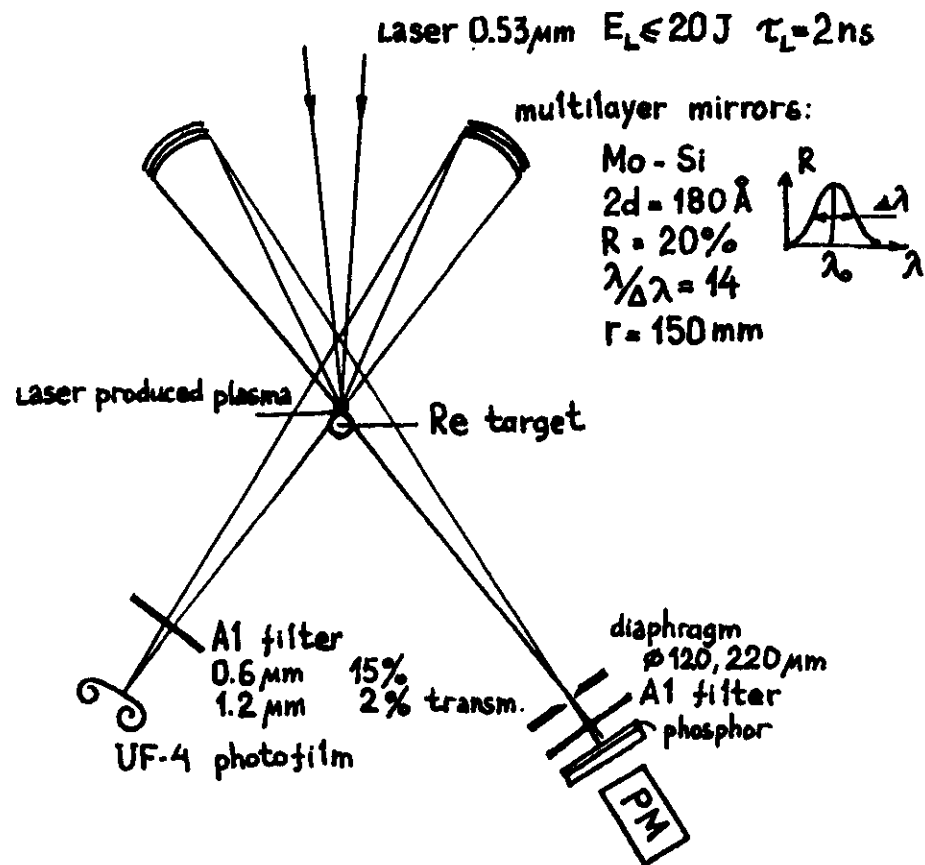
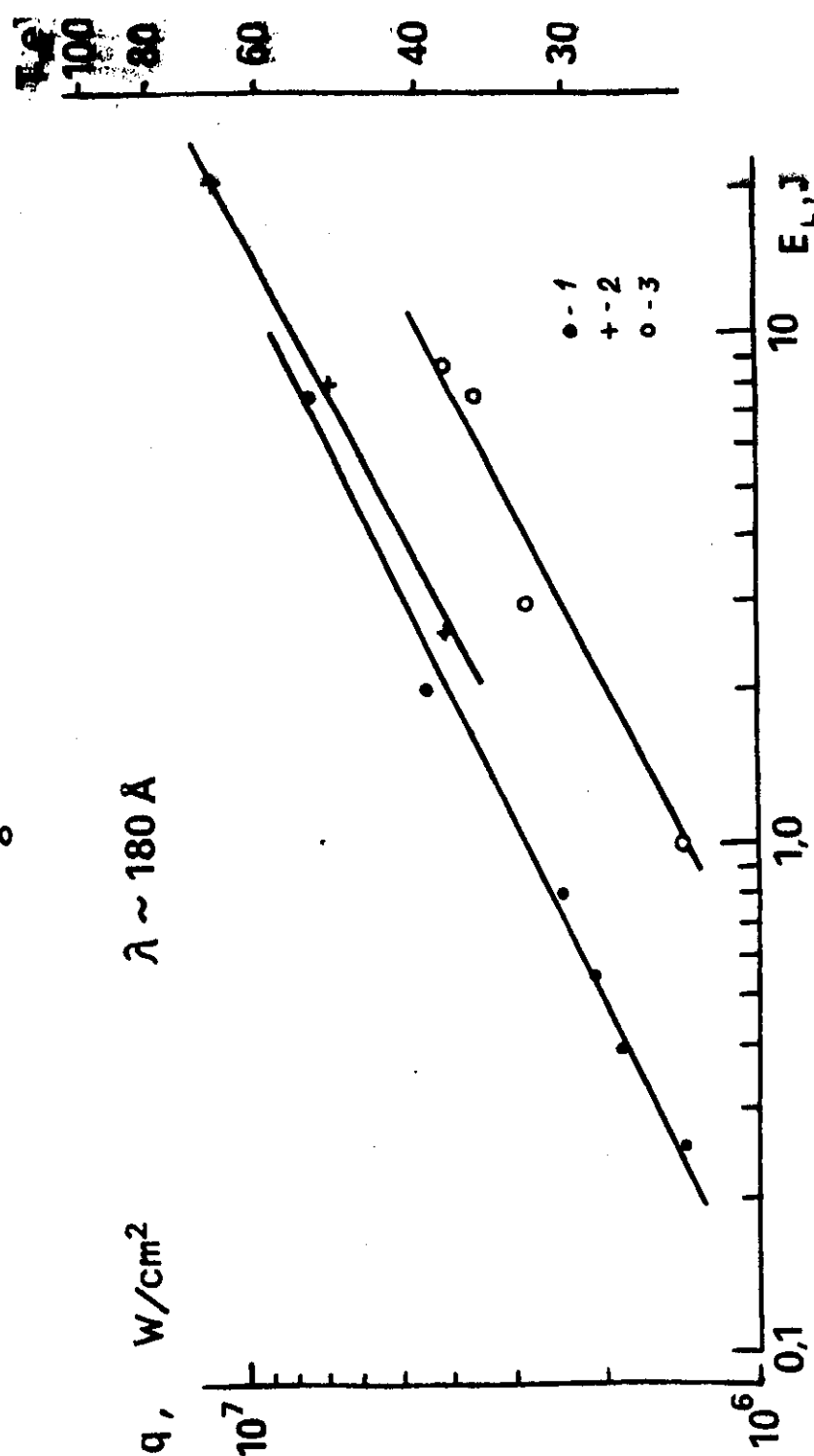


Fig. 14

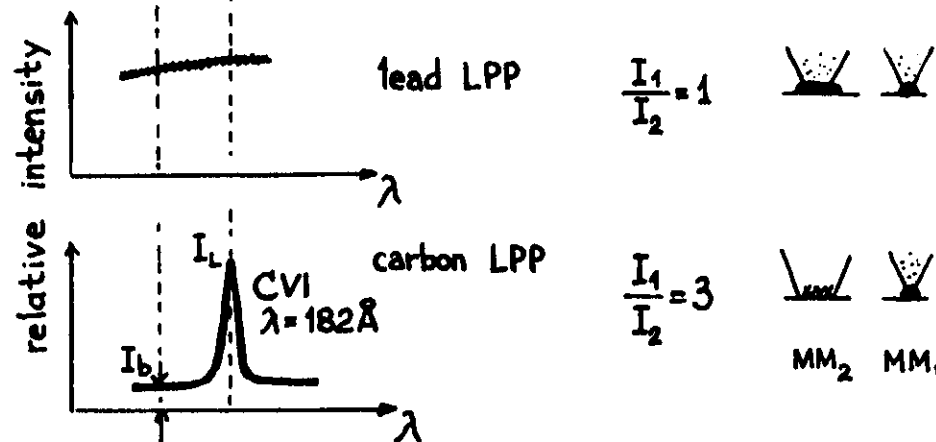
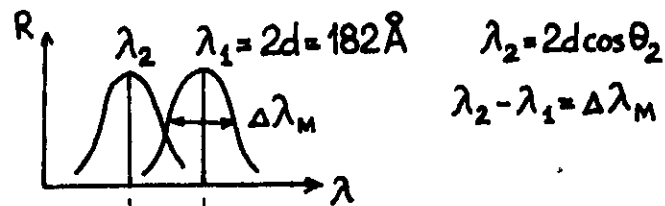
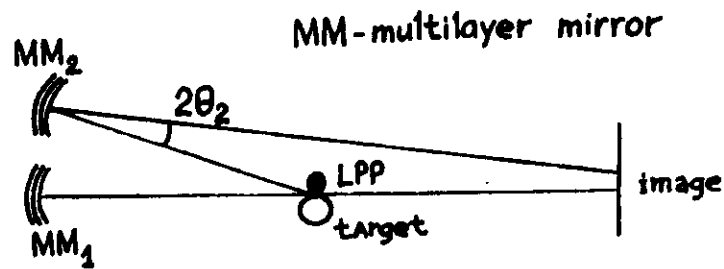
Fig. 15.



The flux density q of the XUV radiation ($\lambda \sim 180\text{\AA}$) and corresponding plasma brightness temperature T

Image of a plasma in the light of spectral line (CVI 3→2 $\lambda 182 \text{ \AA}$)

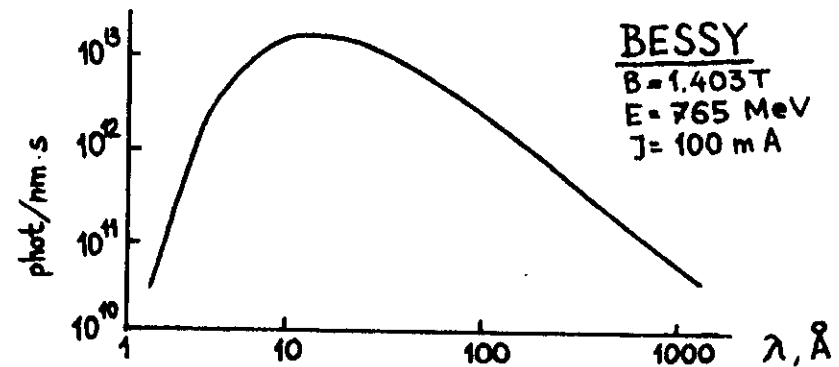
EXPERIMENT:



$$I_L \gg \left(\frac{\partial I_b}{\partial \lambda} \right) \Delta \lambda_M$$

Fig. 16.

Synchrotrons radiation and LPP



spectral photon flux:
for $\lambda = 100 - 200 \text{ \AA}$

SR: $10^{11} \frac{\text{phot}}{\text{\AA} \cdot \text{s}}$ solid angle
 $\Omega = 3 \cdot 10^{-8} \text{ sr}$
(3×3 mm at distance 15 m)

LPP: $5 \cdot 10^{13} \text{ phot/\AA.sr}$

peak power:

SR: repetition rate 10^8 Hz , pulse duration 0.1 ns

$10^{14} \text{ phot/\AA.cm}^2 \cdot \text{s}$

LPP: $1 \times 1 \text{ cm}^2$ at a distance 10 cm from LPP

$5 \cdot 10^{20} \text{ phot/\AA.cm}^2 \cdot \text{s}$

mean (time integral) power:

SR: $10^{12} \text{ phot/\AA.s.cm}^2$

LPP: $(1 \div 5) \cdot 10^{11} (\text{phot/\AA.s.cm}^2) \cdot \nu [\text{repetition rate}]$

for $\nu = 2 \div 10 \text{ Hz}$

$$I_{LPP} = I_{SR}$$

Fig. 17

